THEORETICAL AND EXPERIMENTAL INVESTIGATION FOR THE EFFECT OF STRAIN ON THE BELOW THRESHOLD OUTPUT OF InGaAsP DIODE LASERS

THEORETICAL AND EXPERIMENTAL INVESTIGATION FOR THE EFFECT OF STRAIN ON THE BELOW THRESHOLD OUTPUT OF InGaAsP DIODE LASERS

By

Chen Sheng, M.Sc.

A Thesis

Submitted to the School of Graduate Studies

in Partial Fulfilment of the Requirements

for the degree of

Master of Engineering

McMaster University

September 1992

MASTER OF ENGINEERING(1992) McMaster University
(Engineering Physics) Hamilton, Ontario, Canada

TITLE: Theoretical and Experimental Investigation for the Strain Effect on the Below Threshold Output of the InGaAsP Diode Lasers

AUTHOR: Chen Sheng, M.Sc.(TUNS)

SUPERVISOR: Dr. Daniel. T. Cassidy

NUMBER OF PAGES: vii, 52

ABSTRACT

The effect of strain (stress) on the below threshold output of InGaAsP diode lasers has been investigated theoretically and experimentally.

The degree of polarization (**DOP**) and the polarization-resolved spectral output (**PRSO**) were obtained as a function of the external stress applied to the device. A correlation between the **DOP** and the peak of the **PRSO** as a function of the stress was found. This correlation suggests that below threshold, **DOP** can be used to measure the strain in the active region of lasers. A model based on a strain modified Shockley matrix for the band calculation and a strain modified dipole moment for the optical emission has been constructed to bridge the correlation between the **DOP** and **PRSO**.

ACKNOWLEDGEMENTS:

The author would like to express his gratitude to Dr. D.T. Cassidy for his advice and time during this work to Drs. J. Simmons and J. Preston for their reading and correction for the thesis, and to G. Leinweber and D. Bruce for their kind assistance and useful discussion for the experiment.

I would like to thank my wife and daughter for their understanding and support and the basement people for their useful discussion and kindness.

Table of Contents

List of Figures

Chapter 1

Introduction

The effects of strain on the characteristic of the light output from diode lasers have attracted the interest of laser designers. Effort has been made to investigate the effects both experimentally and theoretically. Stress in the device modifies the band structure, which changes the light output of the device. This strain perturbation, if it is appropriately applied, can enhance the performance of the device, by reducing the threshold current [1,2,3,4], the temperature sensitivity [5,6], line-widths [2,5], and by enhancing light polarization switching [7,8,9,10].

The first experiment results [11] about the effect of strain on diode lasers were given by Ryan and Miller in 1963. They showed the effect of uniaxial compressive strain perpendicular to the junction on the threshold and output of GaAs lasers. The explanations of the relevant experimental results, before the mid 1980s, were based on shallow impurities [12]. The strain effect on the polarized light output (TE,TM) from diode lasers was discussed in the same reference [12]. The stress effect on the optical gain was first explained by Dutta [13]. However, he only considered the change of the effective mass due to strain. It was found [14,15] that the effect of a change in effective mass is

smaller than that of a change in the band gap due to strain. Up to date, some researchers [**16,17**] from the experimental measurements of the effect of strain on the band structure and light output gave ambiguous explanations for heavy hole band and light hole band with respect to TE and TM light output of the laser.

Theoretical investigations of the effect of strain on semiconductor band structure have been progressing. Pikus and Bir [**18**] used a coordination transformation (**CT**) to find an expression for the strain perturbation term. They found a very complicated strain modified energy expression for the J=3/2 bands. Later work [**4,15,19**] showed an enrichment of CT method by using further understanding of semiconductors and the computational technology. A theoretical model [**20**] of the effect of strain on the band structure was not very satisfyingly constructed, although it was the best approach to date. The 4×4 Hamiltonian matrix (Shockley matrix) was only analytically diagonalized into a 2×2 matrix.

The conventional experimental technique to measure strain in a device is to measure the spectrally-resolved (**SR**) light from the device by using photo-luminescence (**PL**) or electro-luminescence (**EL**) [**21**]. The peak position and the half width of the PL spectra reveal information [**14**] about the lattice mismatch which is directly related to strain in the material. The comparison, between the measurements of PL spectra and of the x-ray double-crystal diffraction which provides a direct

measure of lattice mismatch, confirms the utility of PL spectra to measure strain. Measuring the polarization resolved spectral output (**PRSO**) is a recent technique [**22**] which reveals more information from the crystal structure. Because the light is both spectrally and polarization resolved before it reaches a detector, only a small fraction of the light is detected. To improve the signal to niose ratio, the intensity of the SR and PRSO light has to be increased. Once the light level is increased, many more electronic transitions occur away from k=0 [**4,23,24**]. So, in this case, using SR and PRSO light from EL or PL is not a real measure of band gap, strain, or lattice mismatch. How can we have a better perception and understanding of the strain and corresponding measurements? Is there any other method to reveal the strain effect in the material without requiring too much unwanted information?

Experimentally, there is another discovery to measure strain, the Degree Of Polarization (DOP) measurement [**1,7,8**]. DOP is defined by:

$$DOP=\frac{TE-TM}{TE+TM} \qquad (1)$$

where TE or TM is the measure of the total polarized light whose polarization is parallel or perpendicular to laser junction plane. If the crystal is stress free (ϵ=0), DOP=0, from the symmetry of the crystal. Tensile stress along TE polarization in the laser reduces DOP while the compressive

stress increases DOP. From measuring the total polarized light of TE and TM, DOP, the normalized index, gives the state of polarization of the light emitted from a device. It has been found in the experiment that DOP is proportional to external stress applied to the device. Since TE light or TM light is an integration of the SR light to the particular polarization, the light from EL or PL needed for the detection can be greatly reduced and the influence of the measuring carriers to the true experimental results can be reduced to much smaller ratio. With a complete understanding of the DOP, one can use it as a strain indicator to substitute the measurement of the SR and PRSO light of PL or EL at low light level, where the measurement of the SR and PRSO light cannot be resolved. Therefore, theoretical understanding and experimental confirmation are necessary to investigate the relationship between DOP and strain and between DOP and SPP (**S**pectrally and **P**olarization resolved light **P**eak) at the intensity resovlable areas of light for SPP.

In this thesis, strain effects on the output of diode lasers are investigated. A theoretical derivation and semi-classical modelling of luminescence is given in chapter 2. The semi-quantum theory of the luminescence will also be discussed in that chapter. In chapter 3, a strain modified Hamiltonian, and the energy levels, effective masses, and wave functions at k=0 are given for a specified direction in order to compare the results with experiment. There is a brief discussion about

the introduction of the strain perturbation Hamiltonian at the beginning of the chapter. The determination of the polarization of the emitted light from the matrix elements is also given. The stress distribution introduced by the probe and two point mounting system is discussed at the end of the chapter 3. The discussion about shear stress is given in addition to the bending stress. In chapter 4, the verification of the validity of using DOP and the experiment error which limits the DOP measurement are presented. Experimental results of DOP and SPP from EL measured at the same temperature, laser current, and stress for 3 different kinds of lasers (Gain guided (GG), Index guided (IG), Ridge waveguided (RG)) are presented in this chapter. The relationship between DOP and SPP is concluded from both experiment results and theoretical derivation. The consistency and discrepancy between the theoretical derivation and the experimental measurements is also discussed in this chapter. A summary of the results and suggestion for further work is presented in chapter 5.

Chapter 2

Theory I : Light Emission Model

2.1 Semi-Classical Model

The spontaneous-emission rate and absorption rate for photons in a semiconductor can be calculated by using time-dependent perturbation theory and summing over the available electron and hole states. A photon of energy $E = E_i - E_f$ is emitted when an electron makes a transition from an initial state E_i to a final state E_f. The transition probability or the emission rate , for the two level system, can be obtained [25,26]:

$$W = \frac{2\pi}{\hbar} |H_{if}|^2 \rho(E_f) \delta[E-(E_i-E_f)] \qquad (2)$$

where $|H_{if}|$ is the matrix element $|\langle i|H'|f\rangle|$ of the time-independent part of the perturbation Hamiltonian between the initial state $|i\rangle$ and final state $|f\rangle$; $\rho(E_f)$ is the density of the final state. It can be both electron and photon state.

After considering the photon-electron interaction, the final state of the optical field and electrons, the occupation probability of electrons and holes on the energy bands, the valence bands degeneracy, conservation of crystal momentum, the rate of spontaneous emission can be derived

[26,27,28]:

$$r_{sp} = A_s\, E \sum_{nm} \int dk\, |P_{nm}(k)|^2\, \delta[E-(E_i-E_f)]\; f_n(E)\; (1-f_m(E)) \tag{3}$$

where, n and m represent the upper and lower energy respectively; $A_s = \frac{4\pi e^2 \bar{\mu}}{m_0^2 \epsilon_0 h^2 c^3}$; $E = \hbar\omega$; $\bar{\mu}$ is the index of refraction; $f_n(E)$ and $(1-f_m(E))$ are the occupation probability of electrons and holes. Since our interest is focused on low light level transitions, the expression for non-degenerate case is used; k is the crystal momentum; $|P_{nm}(k)|$ is the momentum matrix element. It determines light emission between bands and the polarization of the emitted light (determination of polarization from the matrix element will be discussed in the next chapter). In non-degenerate case, $k \approx 0$ is a good approximation.

To keep the discussion simple and clear, consider the emission of light for the electronic transition from conduction band to heavy hole band and to light hole band separately at $k \approx 0$ for the non-degenerate case.

1) Conduction band to heavy hole band (C-HH):

$$\begin{aligned} r_{sp(c,hh)} &= A_s\, E\, |P_{c,hh}|^2\; f_c(E)\; [\,1-f_{hh}(E)\,] \int d^3\boldsymbol{k}\; \delta[E-(E_c-E_{hh})] \\ &= A_s\, |P_{c,hh}|^2\; e^{\frac{\Delta E_f}{k_B T}}\; 2\pi\; \left(\frac{2m_{rh}}{\hbar^2}\right)^{\frac{3}{2}}\; E\; (E-E_g^{(h)})^{\frac{1}{2}}\; e^{-\frac{E}{k_B T}} \end{aligned} \tag{4}$$

where, ΔE_f is the energy difference of quasi-Fermi levels; k_B is Boltzmann constant; E_g is band gap between the bottom of

conduction band and the top of heavy hole valence band; $\frac{1}{m_{rh}} = \frac{1}{m_c^*} + \frac{1}{m_{hh}^*}$.

2) Conduction band to light hole band(C-LH):

$$r_{sp(c,lh)} = A_s \left|P_{c,lh}\right|^2 e^{\frac{\Delta E_f}{k_B T}} 2\pi \left(\frac{2m_{rl}}{\hbar^2}\right)^{\frac{3}{2}} E \left(E - E_g^{(l)}\right)^{\frac{1}{2}} e^{-\frac{E}{k_B T}} \quad (5)$$

where: $\frac{1}{m_{rl}} = \frac{1}{m_c^*} + \frac{1}{m_{lh}^*}$

Taking the derivative in (4) or (5) with respect to E, the position of the peak of the spontaneous emission can be found:

$$E\big|_{peak} = \frac{1}{2} E_g + \frac{3}{4} k_B T + \frac{E_g}{2} \sqrt{\left(1 + \frac{3}{2} \frac{k_B T}{E_g}\right)^2 - 4 \frac{k_B T}{E_g}} \quad (6)$$
$$\simeq E_g + \frac{1}{2} k_B T \qquad (k_B T \ll E_g)$$

It is important to note that the peak position of the spontaneous profile is a linear function of the band gap E_g, if E_g is much larger than $k_B T$.

When the integration of (4) or (5) is performed, the total light of the transition from the given bands can be obtained.

$$R_{sp} = \int_{E_g}^{\infty} r_{sp}\, dE$$

$$= A_s \left|P_{c,(i)h}\right|^2 e^{\frac{\Delta E_f}{k_B T}} 2\pi \left(\frac{2m_{r(i)}}{\hbar^2}\right)^{\frac{3}{2}} \int_{E_g}^{\infty} E\,(E-E_g^{(i)})^{\frac{1}{2}}\, e^{-\frac{E}{k_B T}}\, dE \quad (7)$$

$$= A_s \left|P_{c,(i)h}\right|^2 e^{\frac{\Delta E_f}{k_B T}} 2\pi \left(\frac{2m_{r(i)}}{\hbar^2}\right)^{\frac{3}{2}} (k_B T)^{\frac{3}{2}} \frac{\sqrt{\pi}}{2} E_g^{(i)}\, e^{-\frac{E_g^{(i)}}{k_B T}}$$

(i) = h (heavy hole) or l (light hole)

It can be seen that

$$R_{sp} \propto E_g\, e^{-\frac{E_g}{k_B T}} \quad (8)$$

Within a range of E_g, R_{sp} and the peak position of r_{sp} are linearly related as shown from (6) and (8). This relation can be generalized into the relation of the particular bands transition and/or of the particular polarization.

2.2 Semi-Quantum Theory of the Luminescence

It is well accepted that light emission is due to the oscillation of dipole moments whose vector summation constructs the polarized field in the material [**29**]. The dipole moment matrix element appears in the density matrix formulation [**30,31**] as a vector. The projection of the **E** field along the vector determines the luminescence of the emission mode.

$$|\boldsymbol{M}| = |\langle \phi_{ck} | e\boldsymbol{r} | \phi_{vk'} \rangle| = \frac{\hbar e}{m_0} \frac{1}{E_{cv}} |\langle \phi_{ck} | \boldsymbol{p} | \phi_{vk'} \rangle| \delta_{kk'} \quad (9)$$

The luminescence of light can then be obtained:

$$\Delta I \propto |\boldsymbol{M}_{cv}|^2 = \left(\frac{\hbar e}{m_0}\right)^2 \frac{1}{E_{cv}^2} |\langle \phi_{ck} | \boldsymbol{p} | \phi_{vk} \rangle|^2 \quad (10)$$

The expression (9) for the dipole moment corresponds to the cross term in the density matrix theory [**31**]. It is still not clear what the exact expression for the light emission should be before the consideration of quantization of electrical-magnetic field [**30,31**]. Further discussion is out of the scope of this project. However, it is needed to present the theory here, that the luminescence depends upon the band gap and band shape from the quantum point of view.

The density matrix method is convenient in handling the effect of stress because it takes into account the energy band structure and the transition dipole moment which are both stress-dependent.

2.3 Spectral Broadening of the Light

The above 2 models of the light emission were for the case of "pure" emission. Experimental evidence indicates that there is a decay in the material. This decay phenomenon, similar to the damping terms in a damped harmonic oscillator

model, is intrinsic in the material. It is not known what the strength of this broadening is, although the expression of Lorentz broadening for the decay was given [**30,31**]. This broadening mechanism is used to explain the slow reduction of the spectrum near the band edge transition, since for intrinsic material, it is not satisfied with the explanation of the slow reduction by using the band-tail theory (k not conservative transition) [**26,30**].

$$g(\omega) = \frac{b^2}{(\omega - \omega_0)^2 + b^2} \qquad \textbf{(11)}$$

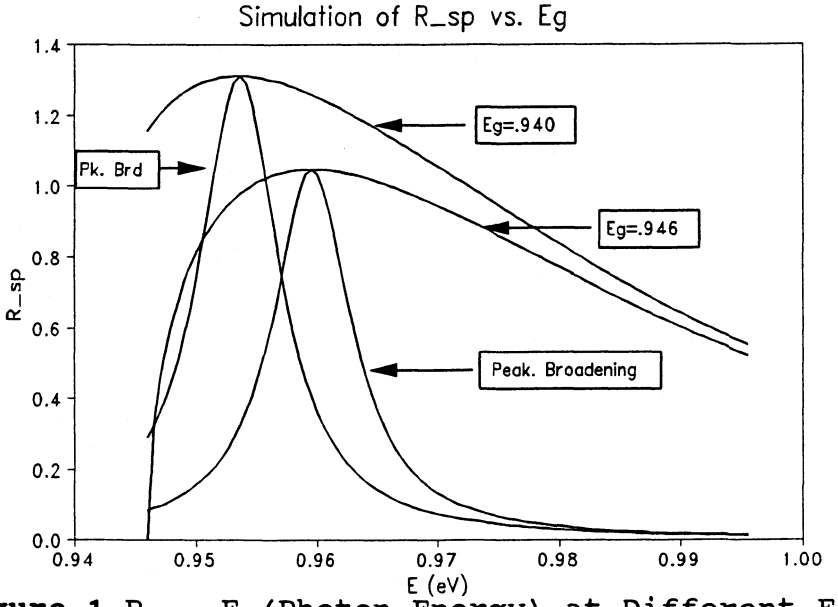

Figure 1 R_{sp} ~ E (Photon Energy) at Different E_g

Since there is no k or strain term in the broadening expression, the effect of strain on this broadening can be ignored. The theoretical light emission spectral profile is

plotted in Figure 1. The broadening was only plotted, in the graph, for the peak position. It is clear that the peak of the spectrum shifts to smaller frequency, when the band gap is reduced.

2.4 Losses in Semiconductor

The experimental output of the spectral profile is given in Figure 2.

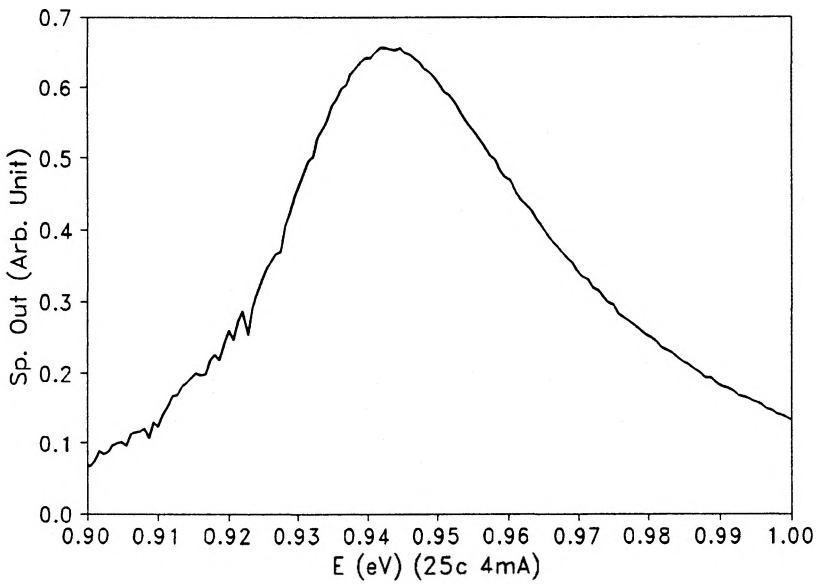

Figure 2 A Typical Spectral Profile from the Experiment

It is apparent that there is a discrepancy at higher frequencies. This can be explained with the absorption. The higher frequency region is most probable region for absorption to take place [**26,29**]. It is not known theoretically how much the absorption affects the light output when stress (or

strain) is continuously added to the device. One has to determine this effect from experiment. In the models given above, the assumption of a weak dependence of absorption on strain is used since the absorption occurs well above the band edge. The experimental results are consistent with the assumption.

2.5 About the Model

After considering the effect of strain to the spectral broadening and the losses, it is appropriate to use the semi-classical model to describe the effect of strain on the low level light output from semiconductor materials. From (6) and (8), the spectral peak and the total light are related directly to the band gap E_g. The next task is to investigate the effect of strain on the band structure.

Chapter 3

Theory II: Band Calculation for a Stressed Crystal

3.1 The Background of Band Theory and Strain Hamiltonian

From Bloch theorem in solid state physics, the Schrödinger equation is:

$$H_0 \psi = [\ \frac{P^2}{2m_0} + V(\boldsymbol{r})\ ]\ \psi = E\psi \qquad (12)$$

where, $V(\mathbf{r})$ is the periodic potential of the crystal; m_0 is the electron mass; E is the electron energy; $p^2/2m_0$ is the kinetic energy of electron; ψ is the wave function of electron. The wave function of the electron in the crystal has the form of $\psi_{\boldsymbol{k}}(\boldsymbol{r}) = e^{i\boldsymbol{k}\cdot\boldsymbol{r}} u_{\boldsymbol{k}}^0(\boldsymbol{r})$; $u_{\mathbf{k}}^0(\mathbf{r})$ is periodic with the periodicity of the lattice and has the symmetric characteristic of the crystal. It modulates the wavefunction of free electron.

Based on the results of cyclotron resonance and insights from Group Theory based on the symmetry considerations of the crystal [32,33,34,35,36], it is known that the conduction band is S like and the valence bands are P like with 3 fold degenerate (if the spin of the electrons is considered, there are 6 fold degenerate) in III-V semiconductor materials. The modulation functions (they will

be called, for simplicity, wave functions because they are part of Bloch wave functions and the wave function of free electron gives a Delta function as far as the action of Hamiltonian is concerned), $u_k^0(\mathbf{r})$, have the following symmetry properties: |S> is completely symmetric in x, y, and z direction, |X> is antisymmetric in x direction but symmetric in y and z direction; |Y> is antisymmetric in y direction but symmetric in z and x direction; |Z> is antisymmetric in z direction but symmetric in x and y direction. These four functions look like S electron and P electrons in the description of hydrogen atoms.

When spin-orbit interaction is considered [37,38], the perturbed Hamiltonian is:

$$H = H_0 + H_1 = \frac{p^2}{2m_0} + V(\boldsymbol{r}) + \frac{1}{4m_0^2c^2}[\sigma \times \nabla V(\boldsymbol{r})] \cdot \boldsymbol{p} \qquad (13)$$

E	$\langle J\rangle$ $\langle m_J\rangle$	u_i
E_c:		$S\uparrow$
E_c:		$S\downarrow$;
E_{hh}:	$\left\|\frac{3}{2}\ \frac{3}{2}\right\rangle =$	$\frac{1}{\sqrt{2}}(X+iY)\uparrow$
E_{hh}:	$\left\|\frac{3}{2}-\frac{3}{2}\right\rangle =$	$\frac{i}{\sqrt{2}}(X-iY)\downarrow$;
E_{lh}:	$\left\|\frac{3}{2}\ \frac{1}{2}\right\rangle =$	$\frac{i}{\sqrt{6}}[(X+iY)\downarrow-2Z\uparrow]$
E_{lh}:	$\left\|\frac{3}{2}-\frac{1}{2}\right\rangle =$	$\frac{1}{\sqrt{6}}[(X-iY)\uparrow+2Z\downarrow]$;
E_{sp}:	$\left\|\frac{1}{2}\ \frac{1}{2}\right\rangle =$	$\frac{1}{\sqrt{3}}[(X-iY)\downarrow+Z\uparrow]$
E_{sp}:	$\left\|\frac{1}{2}-\frac{1}{2}\right\rangle =$	$\frac{i}{\sqrt{3}}[-(X-iY)\uparrow+Z\downarrow]$.

(14)

The energy and wave functions modified by the spin-orbit interaction, at $k=k_0=0$, are given in (14) [**34,39,40**]. In (13) and (14), σ is the Pauli spin matrices; The six fold degenerate valence bands are decoupled into the four fold degenerate bands (heavy hole and light hole) and the two fold degenerate bands (split-off) under the perturbation of spin-orbit interaction; E_c is the energy of conduction band, E_{hh} is the energy of the heavy hole band, E_{lh} is the energy of the light hole band, and E_{sp} is the energy of the split-off band; $E_{hh}=E_{lh}$; the band gap energy, $E_g=E_c-E_{hh}$; the energy difference between hole bands and split-off bands, $\Delta_{sp}=E_{hh}-E_{sp}$. For the quaternary materials of InGaAsP/InP, $\Delta_{sp}/E_g \approx 1/3$. u_i are the modified wavefunctions by the spin-orbit interaction. Because

the split-off bands are far away from the conduction bands, their contributions for light emission of electron transitions from conduction bands to valence bands and for the interaction among the valence bands may not be taken into account. The problem can be approached by using the first six wave functions of (14).

When the crystal is experiencing a relatively small deformation, the effect of the deformation (strain) can be considered as a perturbation. There are three ways, to my knowledge, to introduce the strain perturbation into the Hamiltonian:

{1} Pikus and Bir [18] used a coordinate transformation (**CT**) method to obtain the strain perturbation expression for the hole bands (4×4 matrix). They solved the strain modified Shockley matrix and obtained a complicated energy expression for the hole bands:

$$E_{\pm}=Ak^2+a\Delta\pm\sqrt{E_k+E_\epsilon+E_{\epsilon k}} \qquad (15)$$

where:

$$\begin{cases} E_k = B^2k^4+C^2\left(k_x^2k_y^2+k_y^2k_z^2+k_z^2k_x^2\right) \\ E_\epsilon = \frac{1}{2}b^2\left[\left(\epsilon_{xx}-\epsilon_{yy}\right)^2+\left(\epsilon_{yy}-\epsilon_{zz}\right)^2+\left(\epsilon_{zz}-\epsilon_{xx}\right)^2\right]+d\left(\epsilon_{xy}^2+\epsilon_{yz}^2+\epsilon_{zx}^2\right) \\ E_{\epsilon k} = Bb\left[3\left(k_x^2\epsilon_{xx}+k_y^2\epsilon_{yy}+k_z^2\epsilon_{zz}\right)-k^2\Delta\right]+2Dd\left(k_xk_y\epsilon_{xy}+k_yk_z\epsilon_{yz}+k_zk_x\epsilon_{zx}\right) \end{cases}$$

k_i is the element of crystal momentum vector; $k^2=k_x^2+k_y^2+k_z^2$; ϵ_{ij} is the element of strain tensor; $\Delta=\epsilon_{xx}+\epsilon_{yy}+\epsilon_{zz}$; A, A, B, B, C, C, D are the valence band parameters, a, b, and d are the

deformation potential. These parameters are chosen from the data books [41] for the band calculations. Using this method, the strained valence bands' shape and relative position to unstrained case can be obtained; "+" corresponds to light hole band and "-" corresponds to heavy hole band.

{2} Hensel and Feher [42] constructed a strain Hamiltonian from the consideration of the crystal symmetry:

$$\begin{aligned} H_{st} = & -a(\epsilon_{xx}+\epsilon_{yy}+\epsilon_{zz}) - 3b[(J_x^2-\frac{1}{3}J^2)\epsilon_{xx}+c.p.] \\ & -\sqrt{3}d[(J_xJ_y+J_yJ_x)\epsilon_{xy}+c.p.] \end{aligned} \qquad (16)$$

{3} Pollak's strain Hamiltonian [43] is:

$$\begin{aligned} H_{st} &= H_{e_1}+H_{e_2} \\ H_{e_1} &= -a_1\Delta - 3b_1[(L_x^2-\frac{1}{3}L^2)\epsilon_{xx}+c.p.] \\ &\quad -d\sqrt{3}[(L_xL_y+L_yL_x)\epsilon_{xy}+c.p.] \\ H_{e_2} &= -a_2\Delta \boldsymbol{L}\cdot\boldsymbol{\sigma} - 3b_2[(L_x\sigma_x-\frac{1}{3}\boldsymbol{L}\cdot\boldsymbol{\sigma})\epsilon_{xx}+c.p.] \\ &\quad -\sqrt{3}d_2[(L_x\sigma_y+L_y\sigma_x)\epsilon_{xy}+c.p.] \end{aligned} \qquad (17)$$

where a, b, d; a_1, b_1, d_1; and a_2, b_2, d_2 are the deformation potentials; c.p. means cyclic permutation. By using $\boldsymbol{J}=\boldsymbol{L}+\frac{1}{2}\boldsymbol{\sigma}$, I find the above two expressions, {2} and {3}, of strain Hamiltonian are equivalent for J=3/2 bands (i.e. hole bands), $\boldsymbol{L}\cdot\boldsymbol{\sigma}=1$, and $a=a_1+a_2$, $b=b_1+b_2$, and $d=d_1+d_2$. For J=1/2 bands (i.e. split-off bands), $\boldsymbol{L}\cdot\boldsymbol{\sigma}=-2$ and $a=a_1-2a_2$, $b=b_1+b_2$, and $d=d_1+d_2$. Since most of our interest has been focused on the light emission from the electronic transitions between conduction bands and J=3/2 valence bands, the theory derived

from {2} and {3} are equivalent. It can also be proved, by applying (16) into (14) for E_{hh} and E_{lh} bands, that {1} and {2} are the same at k≈0. The equivalence of {1} and {2} away from k=0 requires further proof. {2} is used as our strain modified Hamiltonian because it is simple and easy to manipulate and the electron transition at low light intensity takes place near k≈0.

3.2 Strain Modified Hole Band Energy and Wave Functions at k≈0

From general textbooks [**44,45**], the relation between stress and strain for isotropic materials can be written as following:

$$\begin{pmatrix}\sigma_{xx}\\ \sigma_{yy}\\ \sigma_{zz}\\ \sigma_{xy}\\ \sigma_{yz}\\ \sigma_{zx}\end{pmatrix} = \begin{bmatrix} C_{11} & C_{12} & C_{12} & 0 & 0 & 0\\ C_{12} & C_{11} & C_{12} & 0 & 0 & 0\\ C_{12} & C_{12} & C_{11} & 0 & 0 & 0\\ 0 & 0 & 0 & C_{44} & 0 & 0\\ 0 & 0 & 0 & 0 & C_{44} & 0\\ 0 & 0 & 0 & 0 & 0 & C_{44}\end{bmatrix}\begin{pmatrix}\epsilon_{xx}\\ \epsilon_{yy}\\ \epsilon_{zz}\\ 2\epsilon_{xy}\\ 2\epsilon_{yz}\\ 2\epsilon_{zx}\end{pmatrix} \qquad \textbf{(18)}$$

The laser materials InGaAsP and InP have a zinc-blended structure which has cubic symmetry. In the active region of semiconductor lasers experiencing stress, it can be considered that an external force is acting on the active region (the 'internal stress' in the lasers can be considered as the stress from the cladding layers or substrate acting on the active region).

For most lasers, the facet is cleaved parallel to [110] plane [**23,46**]. The bending stress, in the experiment, is introduced parallel to the junction plane and perpendicular to the laser cavity. Therefore, the external stress direction is parallel to $[\bar{1}10]$ plane.

The axes are chosen as follows: z axis is perpendicular to the junction plane ([001] direction) and x and y axes are in the junction plane and parallel to [100] and [010] directions. Then the external bending stress, σ, is in the x-y plane and along the direction bisecting the x and y axes. From [**44,45**], $\sigma_{xx}=\sigma_{yy}=\sigma_{xy}=\sigma/2$. From (18):

$$\frac{1}{2}\begin{pmatrix}\sigma\\ \sigma\\ 0\\ \sigma\end{pmatrix}=\begin{bmatrix}C_{11} & C_{12} & C_{12} & 0\\ C_{12} & C_{11} & C_{12} & 0\\ C_{12} & C_{12} & C_{11} & 0\\ 0 & 0 & 0 & C_{44}\end{bmatrix}\begin{pmatrix}\epsilon_{xx}\\ \epsilon_{yy}\\ \epsilon_{zz}\\ 2\epsilon_{xy}\end{pmatrix} \qquad \textbf{(19)}$$

Then,

$$\epsilon_{xx}=\epsilon_{yy}=\frac{C_{11}}{2(C_{11}-C_{12})(C_{11}+2C_{12})}\sigma\ ;\quad \epsilon_{zz}=-2\frac{C_{12}}{C_{11}}\epsilon_{xx}\ ;\quad \epsilon_{xy}=\frac{1}{4C_{44}}\sigma\ ;$$

$\epsilon_{yz}=\epsilon_{zx}=0$. *Let* $\sigma=\dfrac{2(C_{12}-C_{11})(C_{11}+2C_{12})}{C_{11}}\epsilon$, then,

$$\epsilon_{xx}=\epsilon_{yy}=-\epsilon\ ;\quad \epsilon_{zz}=2\frac{C_{12}}{C_{11}}\epsilon\ ;\quad \epsilon_{xy}=\frac{(C_{11}-C_{12})(C_{11}+2C_{12})}{2C_{11}C_{44}}\epsilon \qquad \textbf{(20)}$$

Substitute the above strain expressions into (16), the strain perturbation term has the form of:

$$H_{st}=-a(\epsilon_{xx}+\epsilon_{yy}+\epsilon_{zz})-3b[(J_x^2-\frac{1}{3}J^2)\epsilon_{xx}+c.p.] \\ -\sqrt{3}d[(J_xJ_y+J_yJ_x)\epsilon_{xy}+c.p.] \\ =\delta E_H-\delta E_s(J_z^2-\frac{1}{3}J^2)-\delta E_{sh}(J_xJ_y+J_yJ_x) \qquad (21)$$

where:

$$\delta E_H = 2a\frac{C_{11}-C_{12}}{C_{11}}\epsilon \qquad \delta E_S = 3b\frac{2C_{12}+C_{11}}{C_{11}}\epsilon$$

$$\delta E_{sh} = \frac{\sqrt{3}d(C_{11}+2C_{12})(C_{11}-C_{12})}{2C_{11}C_{44}}\epsilon$$

The wave equation, after considering the strain perturbation, can then be written as:

$$H|u_i\rangle = (H_0+H_1+H_{st})|u_i\rangle$$

$$= (E_0+E_1+\delta E_H)|u_i\rangle + \begin{bmatrix} -\delta E_S & 0 & i\delta E_{sh} & 0 \\ 0 & \delta E_S & 0 & i\delta E_{sh} \\ -i\delta E_{sh} & 0 & \delta E_S & 0 \\ 0 & -i\delta E_{sh} & 0 & -\delta E_S \end{bmatrix} \begin{Bmatrix} u_1 \\ u_2 \\ u_3 \\ u_4 \end{Bmatrix} \qquad (22)$$

where $u_1=|\frac{3}{2}\ \frac{3}{2}\rangle$; $u_2=|\frac{3}{2}\ \frac{1}{2}\rangle$; $u_3=|\frac{3}{2}-\frac{1}{2}\rangle$; $u_4=|\frac{3}{2}-\frac{3}{2}\rangle$.

δE_H is a hydro static energy term. It shifts the energy of the whole system toward one direction, that is, it is symmetric. δE_s is an asymmetric energy term. It moves heavy hole and light hole in opposite directions. δE_{sh} is in the off-diagonal term. It contributes to the interaction among the heavy hole and the light hole bands.

Solving for the energy E, one has

$$E_{\pm} = E_0 + E_1 + \delta E_H \pm \sqrt{\delta E_S^2 + \delta E_{sh}^2} \qquad (23)$$

$E_{\pm}$ is proportional to strain since δE_H, δE_S, and δE_{sh} are proportional to the strain (ϵ). '+' corresponds to light hole while '-' is corresponding to heavy hole. By diagonalizing the matrix in (22), I found a unitary matrix,

$$U = \begin{bmatrix} -\alpha & 0 & i\beta & 0 \\ 0 & \alpha & 0 & i\beta \\ -i\beta & 0 & \alpha & 0 \\ 0 & -i\beta & 0 & -\alpha \end{bmatrix} \qquad (24)$$

$$\alpha = \frac{1}{\sqrt{1+\gamma^2}} \qquad \beta = \frac{\gamma}{\sqrt{1+\gamma^2}} \qquad \gamma = \frac{\delta E_{sh}}{\delta E_S + \sqrt{\delta E_S^2 + \delta E_{sh}^2}} = \frac{\sqrt{\delta E_S^2 + \delta E_{sh}^2} - \delta E_S}{\delta E_{sh}}$$

It can be shown that:

$$UU^+ = U^+U = \begin{bmatrix} \alpha^2+\beta^2 & 0 & 0 & 0 \\ 0 & \alpha^2+\beta^2 & 0 & 0 \\ 0 & 0 & \alpha^2+\beta^2 & 0 \\ 0 & 0 & 0 & \alpha^2+\beta^2 \end{bmatrix} = I \qquad (25)$$

where, I is a 4×4 unit matrix. The total Hamiltonian can be diagonalized by using the unitary matrix:

$$UHU^+ = (E_0 + E_1 + \delta E_H) \begin{bmatrix} 1 & 0 & 0 & 0 \\ 0 & 1 & 0 & 0 \\ 0 & 0 & 1 & 0 \\ 0 & 0 & 0 & 1 \end{bmatrix} + \sqrt{\delta E_S^2 + \delta E_{sh}^2} \begin{bmatrix} -1 & 0 & 0 & 0 \\ 0 & 1 & 0 & 0 \\ 0 & 0 & 1 & 0 \\ 0 & 0 & 0 & -1 \end{bmatrix} \qquad (26)$$

So, the new wave functions can be obtained:

$$|v_i\rangle = U|u_i\rangle = \begin{bmatrix} -\alpha & 0 & i\beta & 0 \\ 0 & \alpha & 0 & i\beta \\ -i\beta & 0 & \alpha & 0 \\ 0 & -i\beta & 0 & -\alpha \end{bmatrix} \begin{Bmatrix} u_1 \\ u_2 \\ u_3 \\ u_4 \end{Bmatrix} \qquad (27)$$

Since $\gamma<1$, one has $\alpha>\beta$. For bi-axial stress on the active region with $\sigma_{xx}=\sigma_{yy}$ and $\sigma_{xy}=0$, one has $\delta E_{sh}=0$, $\epsilon_{xx}=\epsilon_{yy}\neq 0$, $\epsilon_{zz}\neq 0$; and $\gamma=0$, $\alpha=1$, $\beta=0$. This case has been clearly explained in Chong's paper [**15**].

It should be noted that the effect of strain in modifying wave functions is not dominant in the comparison with the effect of strain in modifying the band gap and band shape (effective mass).

1) Because of strain modifying the band shape, the corresponding wave functions should be modified. Although this case was pointed out by Adams [**1**] and the references therein, there is no clear mathematical derivation for the modification of the wave functions with strain. It is artificial that the strain effect is only acting on the interaction between the split-off band and the light hole bands. The heavy hole band is degenerate with the light hole band for stress free materials. So, the interaction between bands should be the same from split-off band to the heavy hole band or the light hole band. Moreover, the interaction between heavy hole band and light hole band should be much stronger than that between the split-off band and the hole band when strain is applied to

lift the degeneracy of the hole bands.

2) From CT method, the effect of strain modified wave function was not taken into consideration. The effect of changing wave function by strain is, at least, a higher order effect.

3) In our experiment, we are measuring the change of light emission from the laser by applying external stress to the laser instead of measuring wave functions of the hole bands.

There are two models in chapter 2 which describe the emission rate and the effect of strain on the light emission. The relation between the dipole moment, $\langle\phi_c|\mathbf{er}|\phi_v\rangle$, and the **p** matrix element $\langle\phi_c|\mathbf{p}|\phi_v\rangle$ is directly related to the transition energy E_{cv}.

Although an exact expression from the quantum model of light emission has not been given, the semi-classical model gives a result consistent with our experimental measurements: **light emission is proportional to the band gap, and the band gap is proportional to the stress (strain) applied.** The first part of the above statement has been given in the previous chapter and the second part is given in the next section.

3.3 The Relation of the Band Shape and Band Gap with Strain

The changes of the band shape and band gap with respect to strain are calculated by using (15) or (23). The expression describing the effect of strain on the band gap, at $k\approx 0$, is [15,20]:

$$E_g = E_c - E_{\pm} = E_{g_0} + \delta E_H^c + \delta E_H \pm \sqrt{\delta E_s^2 + \delta E_{sh}^2} \qquad (28)$$

where E_{g_0} is the stress free band gap; $\delta E_H^c = 2a' \frac{C_{11}-C_{12}}{C_{11}} \epsilon$, is the hydro static shift of the conduction band. Since δE_H^c, δE_H, δE_s, and δE_{sh} are proportional to strain (ϵ), the band gap E_g changes linearly with respect to the strain (ϵ).

Figure 3 shows the band structure of the hole bands under the bi-axial stress without considering the hydro static effect of the strain. U(hh) and U(lh) are the unperturbed bands. Upper V(lh) and lower V(hh) are the bands shifting when the active region is under biaxial tensile strain. Upper V(hh) and lower V(lh) are the bands shifting when the active region is under biaxial compressive strain. It can be seen that tensile strain makes the top band 'lighter' perpendicular to the junction and the band 'heavier' parallel to the junction and compressive strain makes the top band 'lighter' parallel to the junction and the band 'heavier' perpendicular to the junction. This means that compressive strain can enhance TE light emission (hole band lighter in the plane) and tensile strain can enhance TM light emission (hole band lighter along [001]). This graph is the same as the Figs. 2 and 3 given by Chong and Fonstad [**15**] and the conclusions about the effect of strain to the hole bands have been drawn by many theoretical and experimental researchers [**14,15,16,17,19,20**].

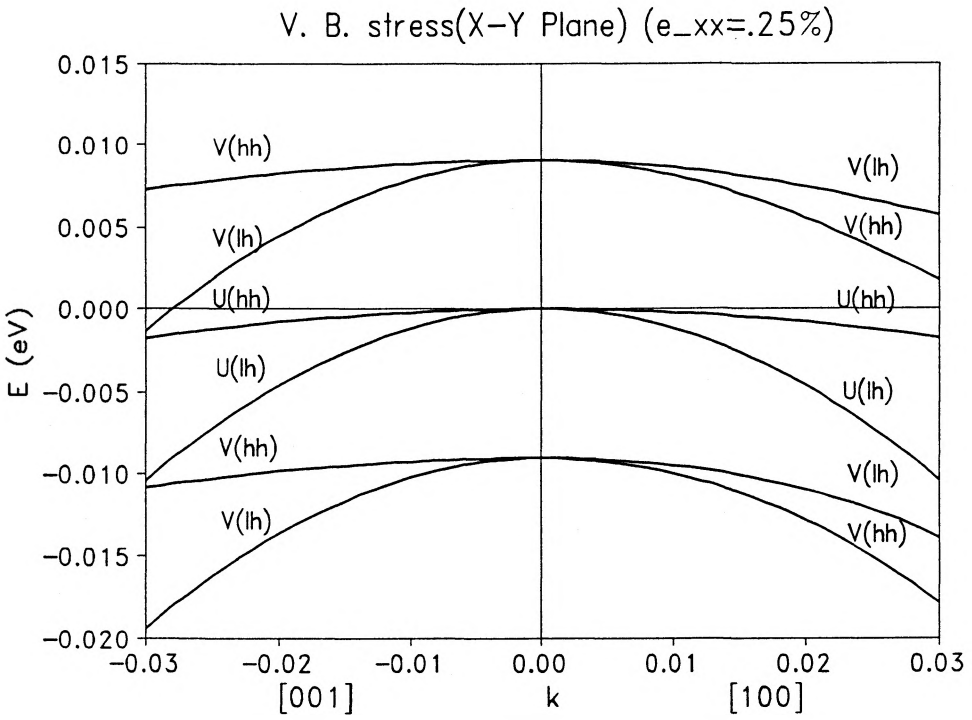

Figure 3 Hole Band Structure under Biaxial Strain

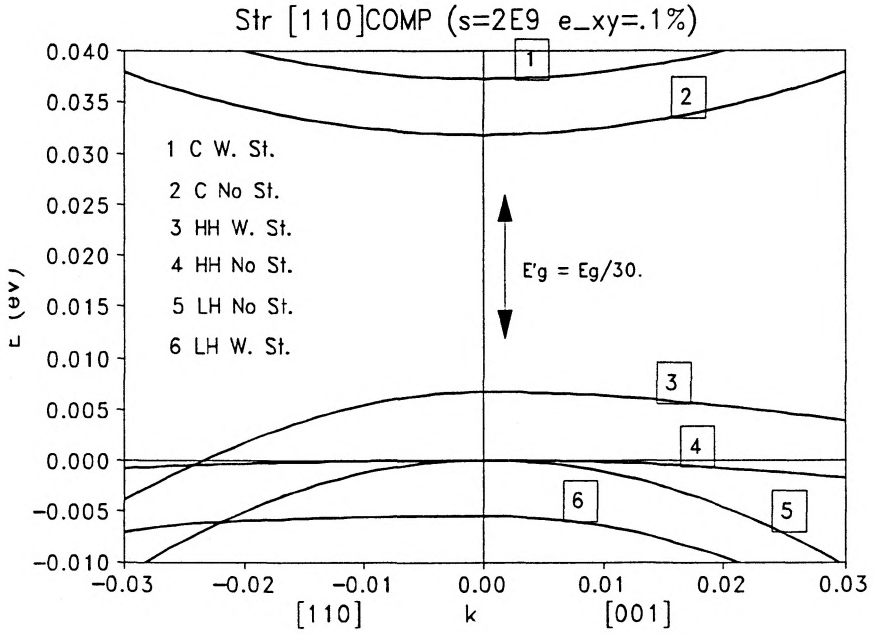

Figure 4 Hole Band Structure with and without Strain for the Compressive Stress along [110]

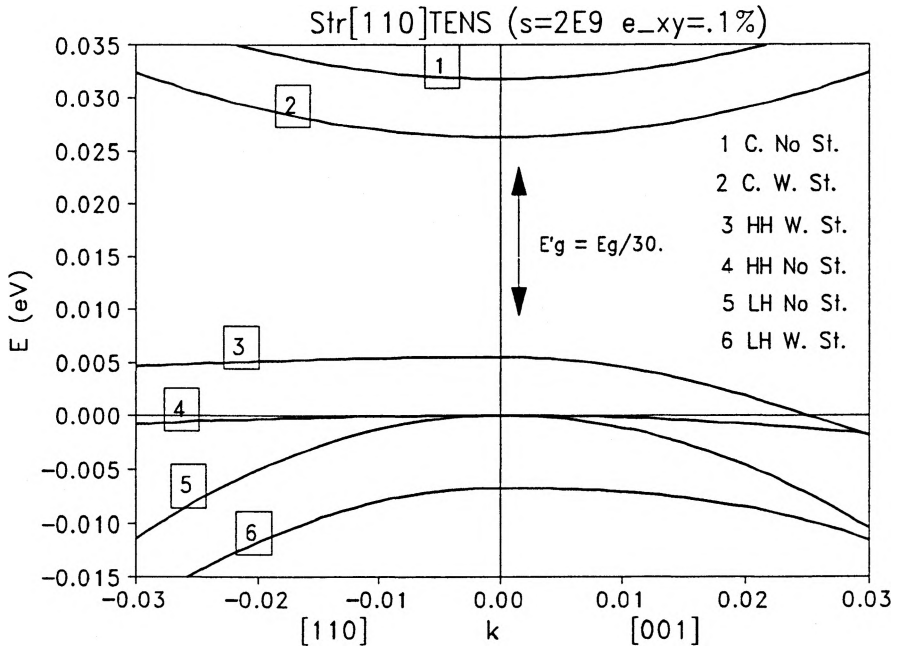

Figure 5 Hole Band Structure with and without Strain for the Tensile Stress along [110]

The contribution of light emission comes from the vector summation of all dipole moments. Doing this summation is very complicated since one has to consider the angular integration to the whole k space. Two particular directions, [001] and [110], are considered here without losing generality.

The band structure is shown in Figure 4 and Figure 5 with and without stress along [110]. It can be clearly seen that: 1) without strain, the hole bands are symmetric in all directions;

2) there are hydro static shifts to the conduction band and hole bands due to strain;

3) at $k \approx 0$, the effective mass of the top band along [110] is increased and the effective mass of the top band along [001] is reduced due to the uniaxial tensile stress. This means the

TM light is enhanced;

4) at k≈0, the effective mass of the top band along [110] is reduced and the effective mass of the top band along [001] is increased due to the uniaxial compressive stress. This means the TE light is enhanced;

5) the motion of the two hole bands with respect to strain is different. The heavy hole shifts much less than the light hole.

3.4 Determination of the Polarization from Matrix Elements

In chapter 2, it was pointed out that the matrix element determines the polarization of the light. This can be proved as follows. The matrix element, $P_{c,(i)h}$ [i= h (heavy hole) or l (light hole)], in the expression of light emission from electronic transition has a form of $P_{c,(i)h}=\langle\phi_c|p|\phi_{(i)h}\rangle$. ϕ_c and $\phi_{(i)h}$ are the wave functions of the conduction band and the hole bands respectively. The polarization of the light is determined by using the action of the matrix element. It should be noted that:

1) the non-zero matrix elements for the transition from the conduction band to valence band are:

$$P_0 = \langle S|p_x|X\rangle = \langle S|p_y|Y\rangle = \langle S|p_z|Z\rangle \qquad (29)$$

The expression for P_0 has been given in the reference [27,39].

2) the polarization of light is determined from the element such that $\langle S|p_x|X\rangle$ has no light polarized parallel to the y-z

plane, $\langle S|p_y|Y\rangle$ has no light polarized parallel to the z-x plane, $\langle S|p_z|Z\rangle$ has no light polarized parallel to the x-y plane. Consider a transition from the conduction band to the $|3/2\ 3/2\rangle$ heavy hole band.

$$|P_{c,hh}|^2=|\langle S|p|\frac{(X+iY)}{\sqrt{2}}\rangle|^2=\frac{1}{2}|\langle S|p_x|X\rangle|^2+\frac{1}{2}|\langle S|p_y|Y\rangle|^2 \qquad (30)$$

It can be seen that, the electron transition from the conduction band to the heavy hole band leads to light polarized only parallel to the junction plane (TE light). For a transition from the conduction band to the light hole band,

$$|P_{c,lh}|^2=\frac{1}{6}|\langle S|p_x|X\rangle|^2+\frac{1}{6}|\langle S|p_y|Y\rangle|^2+\frac{2}{3}|\langle S|p_z|Z\rangle|^2 \qquad (31)$$

The light emitted from this transition has both TE and TM components. This shows that TE light is associated with the electronic transition from the conduction band to both hole bands and TM light arises from the electronic transition from the conduction band to light hole band only. It has been shown from the theoretical calculation (28) and Figs. 4 and 5 that the light hole band moves much faster than the heavy hole band does when an external stress is applied to the laser. This is because the term, δE_s, in the expression for the light hole band has the same sign as the term of δE_H, while that of the heavy hole band has the opposite sign with respect to δE_H. This has been confirmed by the experiment. When the stress is continuously added on the laser, the spectral peak of the TM

light changes much faster than the peak of the TE light as seen in Figure 6. It should be noted that a small fraction of the transitions from the conduction band to the heavy hole band are TM polarized when stress is applied to the laser. (See the derivation of the equation (22)). Since α is much larger than β, the effect from the stress modified transition is very small.

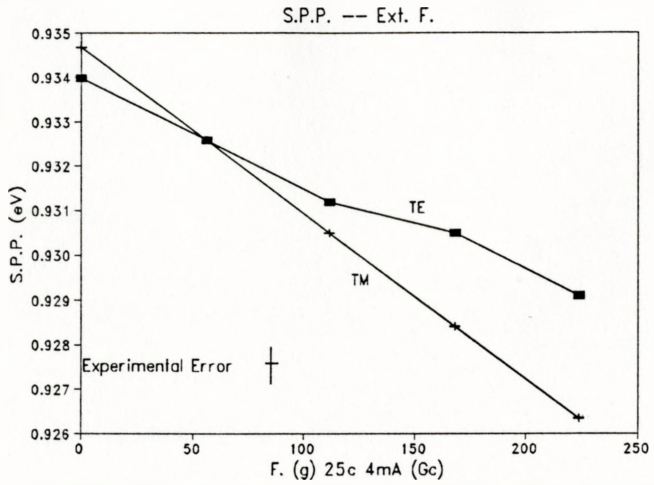

Figure 6 TE and TM Peak Shift under the External Force F at4mA Laser Current and 25°c for a Gain Guide Laser (Gc); (The Experimental Error will be discussed in next chapter)

3.5 Bending and Shear Stress in the Experiment

In the experiment, a flat tapered metal probe is applied on the top of the laser which is sitting on two diamond blocks (or copper blocks) (Figure 7). This system introduces a bending stress along the TE direction to the active region of the laser when there is a weight applied on the top of the

probe. By flipping over the laser (the polarity of the electrical connection can be flipped too), either compressive or tensile stress can be applied to the active region. Temperature control of the laser is achieved through the heat sink which is sitting under the diamond blocks.

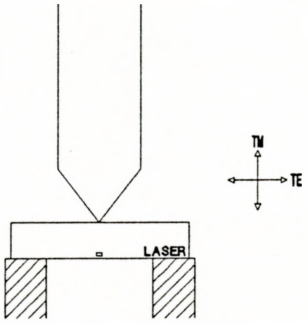

Figure 7 A Probe and Two Diamond Blocks System for Applying External Stress

It has been proved [**47**] that the stress applied to the active region is proportional to the weight (force) applied to the probe. So, the terms the external stress and the external force are inter-changeable. It should be pointed out that there is shear stress perpendicular to the junction in the laser (call it vertical shear stress, for clarity) when the external force is applied perpendicular to the laser junction [**44,45**]. This vertical shear stress is maximum in the central plane and becomes smaller near the top (or bottom) of the chip. Since the active region of the laser is near the top (or bottom) of the chip, this vertical shear stress can be neglected.

Chapter 4

Experimental Results and the Corresponding Explanation

4.1 The Experiment Set-up

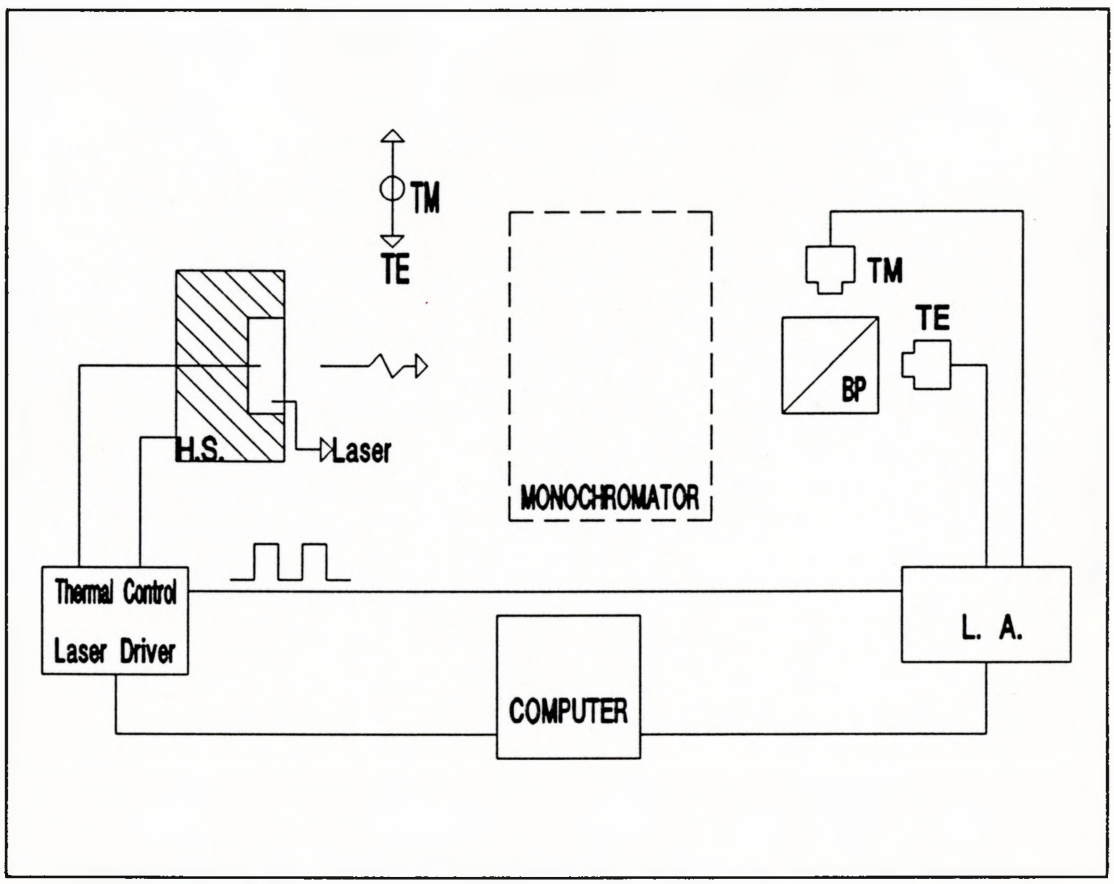

Figure 8 The Schematic of the Experimental Set-up

The system, a probe and two diamond blocks shown in the Figure 7, can introduce external stress and thermal and

electrical contact. The whole experiment set-up is shown in Figure 8. The laser current is electronically modulated in a square wave at 2kHz with 50% duty cycle in order to trigger the lock-in amplifier. A beam split polarizer (BSP) is placed to split TE light and TM light. Two lock-in Evan cards (L.A.) are used to amplify the signal obtained from the two detectors for TE and TM light separately. The frequency of the reference signal for synchronizing the lock-in has the same frequency as the modulation signal with fixed relative phase. A computer was used to control the experimental parameters such as, the laser current level and the heat sink temperature, collecting data, and the motion of the monochromator, and storing the data on the disks for analysis. The monochromator (DIGIKRŌM 240 from CVI laser corporation) was used to resolve the light for the spectral measurement of TE and TM light simultaneous.

SPP was determined from the results of the spectral measurement (using the monochromator) for TE and TM light respectively. DOP was measured without using the monochromator. There are two methods to measure DOP:

a) Putting a detector behind the BSP to measure one polarization of the light (TE or TM); Then by rotating the BSP 90°, the corresponding orthogonally polarized light (TM or TE) can be measured.

b) Using 2 detectors to measure TE and TM at the same time.

It seems that using the second method, b), is simple and can obtain TE and TM signal at the same time. But, one has to

realize that the calibration for the measurement of TE and TM cannot be held all the time because the collimation of the beam through the BSP is not always the same in the actual measurement as in the calibration. This collimation is important to the light split and polarization, especially for TM light, according to the data sheet given by the manufacture [48]. This can also be easily verified in the experiment. For the convenience and the optical instrument available, the first method, a), is used. Since the results were averaged over fifty data points at each measurement, the mean effect of the TE and TM light for the DOP and SPP measurements was obtained.

4.2 Determination of the Laser Current Level for the Measurement

Experimentally, DOP shows a special characteristic as the injection current increases. It can be seen in Figure 9 that: 1) At very low current level (VLCL), DOP is changing fast and not certain as the laser current changes. This fast changing character of DOP at VLCL area was thought, at first, to be the result of the electron transition to a certain band being favoured if there is strain inside the material to split the hole bands. By carefully checking the experiment set-up and the mesurement results, a systematic error was found to be playing the main role in this effect.

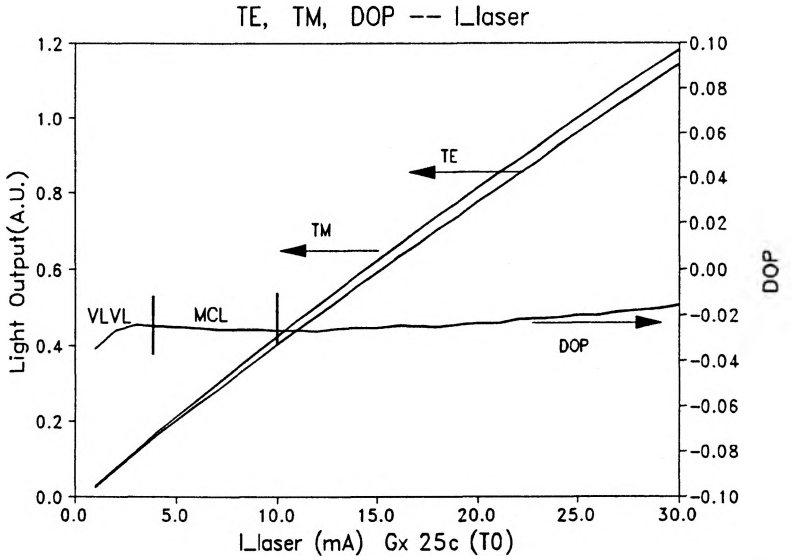

Figure 9 Sample Results from the Experiment for TE, TM and DOP at 25°C and T0 (Tensile Stress ≈0) for a Gain Guide Laser (Gx) at Different Laser Current

This error could be caused by off-collimation of the light beam and/or the non-uniformity of the polarizer. If the calibration error is Q, the measurement of DOP due to the error is:

$$DOP = \frac{TE_0 + Q - TM_0}{TE_0 + Q + TM_0}$$

Let Q=1(mV). If TE_0~10(mV) and TM_0~9.8(mV), DOP≈0.0577;

If TE_0~100(mV) and TM_0~98(mV), DOP≈0.0151;

If TE_0~200(mV) and TM_0~196(mV), DOP≈0.0126.

This abnormal value of DOP at VLCL has been verified in our experiment and simulated in Figure 10.

2) At moderate current level (MCL), DOP is relative constant as can be seen from Figure 9 and Figure 10. This is because TE light and TM light have almost the same increment of the light

emission in the MCL area.

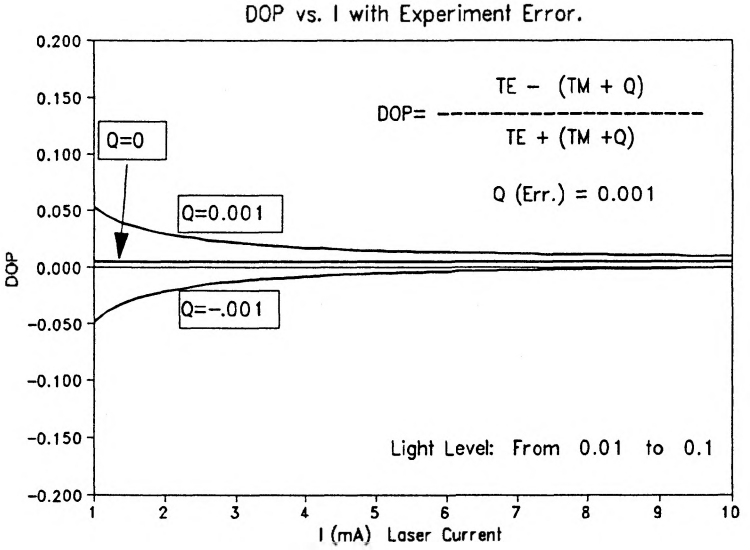

Figure 10 The Effect of the Systematic Error at VLCL

3) For current levels larger than MCL, DOP is changing non-linearly as the current increases, as shown in Figure 9. This phenomenon can be explained using the effect laser current on gain up to this level. The preference of the gain to TE light and TM light is usually different in the laser [**15,16**].

The MCL area has been chosen to investigate DOP and SPP because the relative experimental error is small. For some lasers, there is almost no MCL area. In this case, the smallest available current level was used for the measurement.

4.3 Experimental Results for DOP, SPP and Strain

The experimental error was determined, before the results are presented, as follows:

1) DOP, TE and TM vs. laser current (I). At MCL, DOP does not change too much as the laser current increases (Figure 9).

$$
\begin{aligned}
DOP &= \frac{(TE \pm \Delta TE) - (TM \pm \Delta TM)}{(TE \pm \Delta TE) + (TM \pm \Delta TM)} \\
&\approx \frac{TE - TM}{TE + TM} \pm \left(1 + \frac{TE - TM}{TE + TM}\right) \frac{\Delta TE + \Delta TM}{TE + TM} \\
&\approx DOP_0 \pm \frac{\Delta TE + \Delta TM}{TE + TM} \\
&= DOP_0 \pm \Delta DOP
\end{aligned}
\qquad (33)
$$

From (33), if TE and TM are around 0.25 (V) and ΔTE and ΔTM are around 5.0×10^{-4}, ΔDOP≈0.002. It is quite possible to keep the measurement error smaller than this value for a fixed measuring system. Because the measuring system has to be changed for different lasers and for the different sign of the stress for each laser, ΔDOP is around 0.005. This error of DOP also includes the effect of small temperature fluctuations in the laser.

2) The peak position of the spectral profile was found quite repeatable within 1 nanometre (nm). The wavelength reading from the monochromator at each position can have resolution up to 0.01 nm, so this instrument has very small error contribution to the measurement. The stability of the peak with respect to temperature is about 0.5nm/°C. Since the heat sink temperature can be controlled within ±0.1°C, the instability of the peak position due to the temperature change is within ±0.1 nm. The stability of the peak position with respect to the laser current is within ±0.1 nm because the

peak position shifts within 0.8nm/mA for a typical laser and the laser current can be controlled within ±0.1 mA in the experiment.

3) The error of the external force reading was determined through the experiment. It was found that the error of the weight reading near the situation of the probe touching the laser is relative large. Since one needs the probe to have a complete contact with the laser in order to have a good electrical conduction, the error of the stress corresponding to the external force is relative small (within ±5g) in the experiment. This weight error can introduce the errors of DOP to 0.002 from Figure 11 and of SPP to 0.2 meV (<0.3 nm) from Figure 6.

The above three sources of experiment error are dominant and not easily avoidable. It should be noted that other errors exist. Some have small effect on the measurement and some can be controlled to lower level through the special design of the experiment. For example, averaging 50 data points at one reading point can reduce the error from white noise and the bit error reading of the ADC (analog to digital conversion) system.

In Figure 11 a linear relation of DOP and the external stress (tensile) is shown from the experiment at room temperature and at MCL laser current.

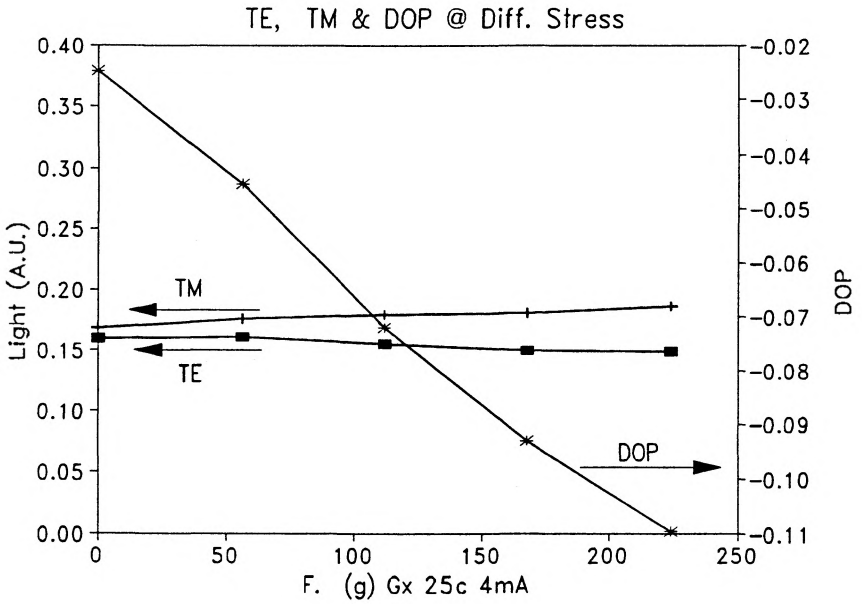

Figure 11 Experiment results of TE, TM, DOP ~ the External Force, F, Applied at 4mA Laser Current and 25°C for a GG Laser (Gc)

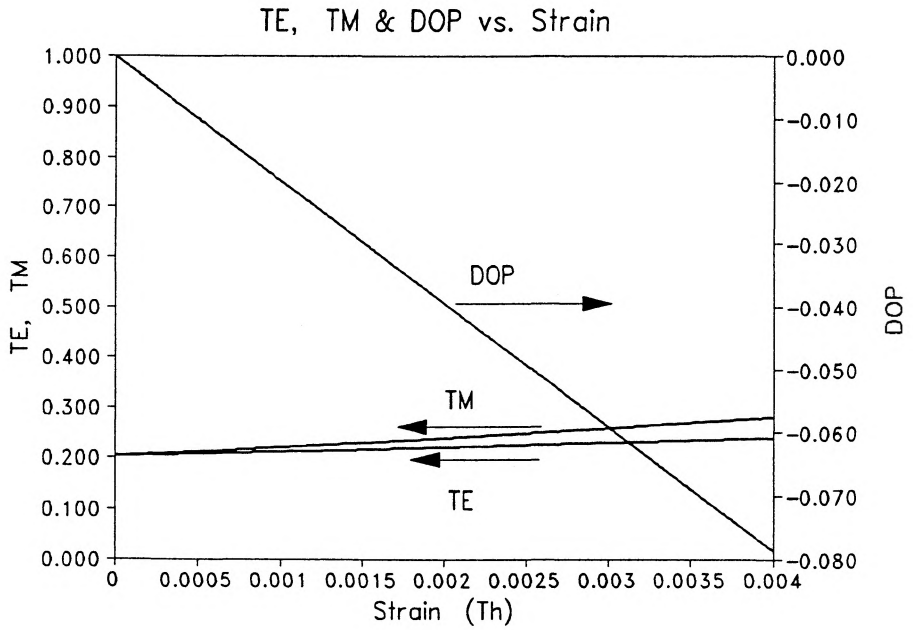

Figure 12 Theoretical Simulation of TE, TM and DOP ~ Strain

As can be seen from this figure, tensile stress reduces the DOP. The theoretical explanation for the results of Figure 11 is shown in Figure 12 by considering the light emission from the conduction band to the light hole band only for TM light and to both light and heavy hole bands for TE light. Although there is a difference in numbers between the experimental results and the theoretical simulation, a linear relation between DOP and stress (strain) in the two figures is clearly explained.

Another theoretical simulation of SPP ~ strain is given in Figure 13 in comparison with the experimental results given in Figure 6.

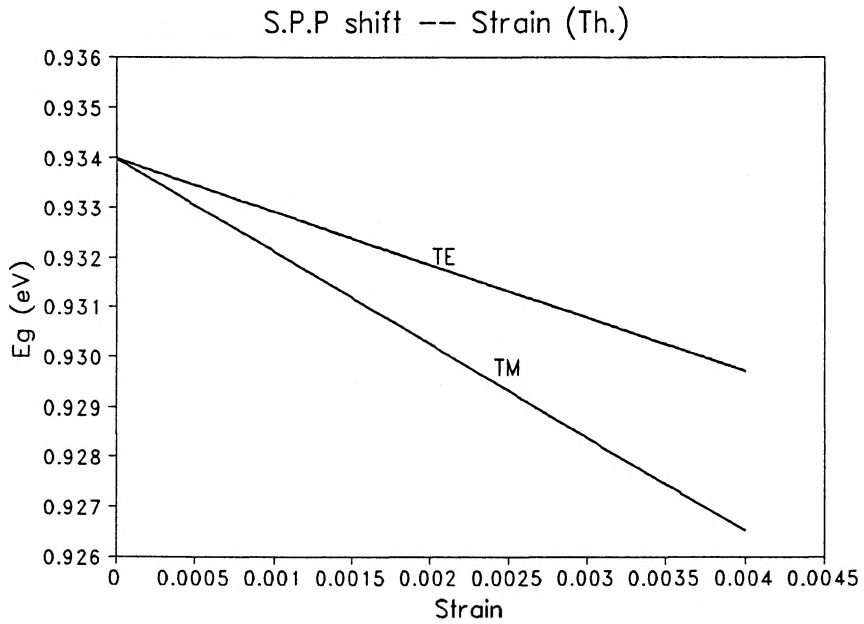

Figure 13 Theoretical Simulation of SPP Shift ~ Strain

It is evident that the SPPs of TE and TM are linearly related to the strain and that the peak of the TM light responds more than that of the TE light. This is consistent with the explanation of band structure given in section 3.3 and 3.4 (Light hole band shifts more than heavy hole band).

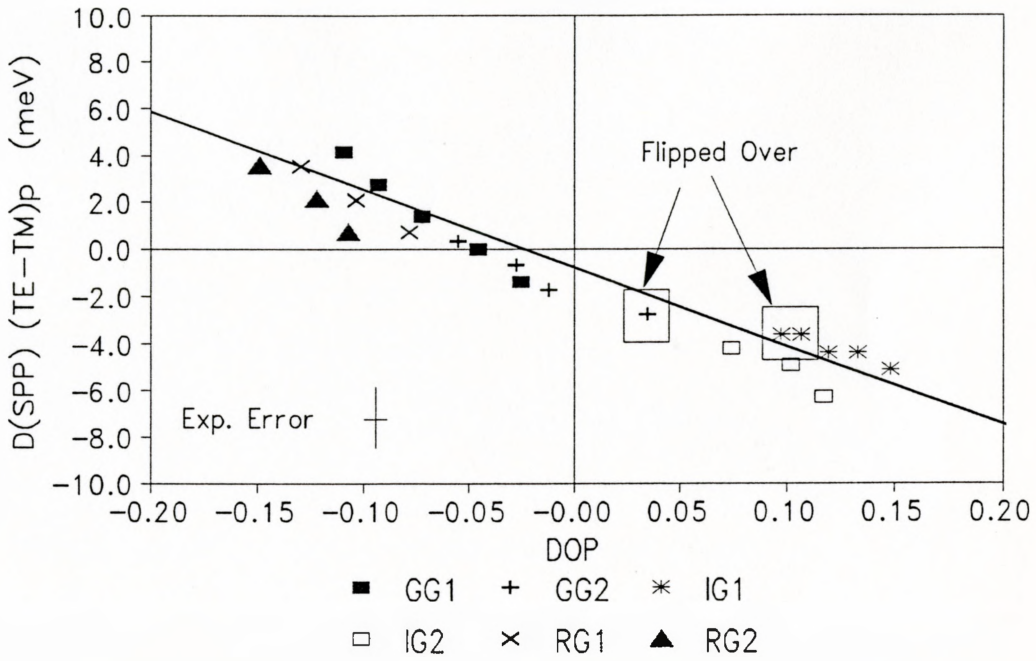

Figure 14 The Relation between DOP and D(SPP)=TE_{peak}- TM_{peak}

Figure 14 gives the relationship of DOP and the difference of SPP between TE and TM light [D(SPP)=TE_{peak}-TM_{peak}]. Three kinds of InGaASP lasers were measured at MCL laser current and room temperature. It is clear that:

1) DOP and D(SPP) have a linear relation.

2) the relation for all three kinds of lasers is linear.

3) When the laser is experiencing tensile strain, DOP<0 and

D(SPP)>0. This is because tensile strain lifts light hole band up and the corresponding band gap is reduced. Since the peak of TE light moves less than that of TM light, D(SPP)=TE_p-TM_p, the difference between TE peak and TM peak increases.

4) When the laser is experiencing compressive strain, DOP>0 and D(SPP)<0. This means compressive strain lifts heavy hole band up and the corresponding band gap is reduced. Since D(SPP)=TE_p-TM_p, the difference between TE peak and TM peak is reduced. When TM_p is larger than TE_p, D(SPP) becomes negative.

5) IG lasers have compressive strain inside, RG lasers have tensile strain inside and GG lasers have very small amount strain.

6) Two lasers were flipped over to measure the stress with opposite sign and they are shown in figure 14. The flipping was performed for the gain guide laser (GG2) from tensile stress (active region bottom) to compressive stress (active region top) and for the index guide laser (IG1) from compressive stress to tensile stress.

7) It seems that at the point D(SPP)=0, there should be DOP=0 because at zero strain, the crystal has perfect cubic symmetry for zinc blende structure. But, the experimental results tell us there is an offset for the intercept point. It needs further investigation.

8) GG lasers can have larger stress response region while IG and RG lasers have smaller stress response region. Since the material for making the lasers is very brittle, most lasers

were broken after certain amount stress was applied.

It can be clearly seen from Figure 14 that DOP and D(SPP) have a single linear relation for these three kinds of lasers in the MCL area. A non-zero intercept is found from the experiment, although the intercept is predicted to be zero from the theory. Further investigation is needed to understand the offset. Although the intercept point is not zero from the experiment, one can still use the DOP measurement to substitute the SPP measurement at MCL area to obtain the measurement results with smaller error (section 4.3) and to determine the D(SPP) from DOP.

Chapter 5

Discussion and Conclusion

5.1 Discussion

Although the correlation between DOP and SPP with respect strain has been found theoretically and confirmed experimentally for InGaAsP diode lasers, there is a discrepancy for the intercept point between the theoretical calculation and the experiment.

Theoretically, if the active region of a laser is stress free, $SPP|_{TE}=SPP|_{TM}$ (i.e. D(SPP)=0) and DOP=0. This can be explained from the cubic symmetry of the crystal. When there is crystal deformation (stress or strain) in the laser, this symmetry is broken and there are non zero results for the measurement of DOP and D(SPP). From the experimental results plotted in Figure 14, if the results are extrapolated to the point of DOP=0, one finds, within the experimental uncertainty, that $D(SPP)\neq 0$. This can be explained as:

1) Experimental Error;

The experimental error is also shown in the Figure 14. The experiments were carried out for three different kinds of lasers and the results fall into the error region along a line. Since for each data point the times of measurements are

not enough to find the mean value and the confident region, it is needed to make more measurements to further confirm if there is the offset, although, in my results, this error does not seem playing a main role for the offset.

2) Spectral Calibration for the Measuring System;

It was found that the throughput of the monochromator and the BSP are different for TE and TM light. The calibration was done by putting a calibrated white light source at the point where the laser was put to calibrate spectral response of the measuring system. Although the whole measuring system was calibrated by using a calibrated light source for TE and TM separately, it is worth examining the system by using different calibration system.

3) Wave Guide Effect;

Since the light is emitted from the active region of the laser, there is a possibility of the wave guide modulating the light output. The index of refraction for the substrate and the top cladding layer is smaller than that for the active region in order to have optical confinement. According to the wave guide theory, the preference of the transmission for TE and TM light in the wave guide is different. Since the laser current is very small, most of the light is emitted from a volume near the facet of the laser because of the absorption. Since it is not known how deep this emission region is, it is too early to decide if the wave guide effect causes the offset for DOP and D(SPP). This wave guide effect can be examined by

using a bare InP bar to replace laser chip to do the same measurements for DOP and SPP as for laser. If there is still an offset for DOP and D(SPP), the wave guide effect for the offset can be ignored.

4) Electrical Field Effect;

In the experiment, bias voltage was applied to the laser to introduce the injection of the laser current. Since the electrical field was applied perpendicular to the junction of the laser, the effect from the electrical field could break the symmetry along the direction of TE and TM for the stress free materials. Further investigation of this effect is needed.

2) and 3) are discussed in using EL method. A PL method can be used to compare the results for DOP measurement between EL and PL method. It should be noted that one has to make sure the PL transitions are from the bottom of the conduction band to the top of hole band by checking the spectral width, if it is measurable.

It has been shown [**44,45,47**] that there is a linear relation between the bending stress (strain) and the force applied. The proportion constant (slope) in the relation depends on the geometrical size. From (3.26) and (3.27) of the reference [**47**], the bending stress in the active region is proportional to w^{-1} and h^{-3} for the same amount of force applied, where w is the cavity length of the laser and h is the thickness of the laser chip. Since the gain guide laser in

the measurement has less cavity length and thickness of the laser, it shows a relative fast stress response in the DOP and D(SPP) plot (Figure 14), comparing to the other kinds of the lasers. Since the geometrical size is different from laser to laser, the corresponding bending stress (strain) which the active region of the laser is experiencing is different for the same amount force applied through the weight on the top of the probe. So, in the theoretical calculation, strain was used and in the experiment results, applied force was used. The actual calibration for the stress inside the active region with respect to the force applied has to be treated on each individual case after the geometrical size of the laser is carefully measured. Using (3.26) of the reference [**47**] and choosing w=250μm, h=100μm with the chip width l=300μm, the active region position away from the top (or bottom) of the chip z=20μm, and the active region position away from the probe, x=30μm, a sample relation of the bending stress with respect to the applied force can be obtained as

$$\sigma \simeq \pm 1.3\times10^{9} F \ (\mathrm{dyn/cm^2}).$$

where, F is the number in Newton.

5.2 Conclusion

The effect of strain on the below threshold output of the lasers was studied. The experimental results show that the

uniaxial compressive stress in the junction plane and perpendicular to the laser cavity increases the light emission with polarization parallel to the junction plane and perpendicular to the bending stress and the tensile stress increases the light emission with polarization perpendicular to the junction plane and the direction of the bending stress. Although the change of the light emission with respect to the stress is not large and depends on the geometry and the internal structure of the lasers, a normalized number DOP was found proportional to the change of the stress (strain) at room temperature. The linear relation between DOP and SPP in a certain range of different stress level was found experimentally for three kinds of lasers and explained theoretically. It is possible, from this work, to say that using the DOP measurement can substitute the SPP measurement. A better sensitivity and resolution for the DOP measurement can be obtained at MCL level comparing to the SPP measurement. After this work, one can have much more confidence to use DOP measurement than before. Part of this work has been presented in the Sixth Canadian Semiconductor Technology Conference in Ottawa in August, 1992 [**49**].

References:

[1] C. S. Adam and D. T. Cassidy, "Effects of stress on threshold, current, and polarization of the output of InGaAsP semiconductor diode lasers", J. Appl. Phys. **64**(12) 6631 (1988)

[2] S. Tiwari, R. S. Bates, C.S. Harder, and A. Behfar-Rad "Effects of compressive and tensile uniaxial stress on the operation of AlGaAs/GaAs quantum-well lasers", Appl. Phys. Lett. **60**(4) 413 (1992)

[3] A.R. Adams,"Band-structure engineering for low-threshold high-efficiency semiconductor lasers", Electron. Lett., **22**(5) 249 (1986)

[4] E. Yablonovitch and E. O. Kane, " Band structure engineering of semiconductor lasers for optical communications", IEEE, J. Lightwave Tech., **6**(8) 1292 (1988)

[5] P.J. Thijs,L.F. Tiemeijer,P.I. Kuindersma,J.J.M. Binsma, and T. V. Dongen, "High-performance 1.5 μm wavelength InGaAs-InGaAsP Strained Quantum Well Lasers and Amplifiers",IEEE J. Quantum Electron., **27**(6) 1426 (1989)

[6] J. Evans, T. Makino, N. Puetz, J. G. Simmons, and D. A. Thompson, "Strain-induced performance improvements in long-wavelength, multiple-quantum-well, ridge-waveguide lasers with all quaternary active regions", IEEE Photon. Tech. Lett. **4**(4) 299 (1992)

[7] M. J. B. Boermans, S. H. Hagen, A. Valster, M. N. Finke J. M. M. Van Der Heyden, "Investigation of TE and TM polarised laser emission in GaInP/AlGaInP lasers by growth-controlled strain", Electron. Lett., **26**(18) 1438 (1990)

[8] D.T. Cassidy and C.S. Adam, "Polarization of the output of InGaAsP semiconductor diode lasers",IEEE, J. Quantum. Electr., **25**(6) 1156 (1989)

[9] J. Liu and Y. Chen, "Compensation of internal thermal stress in InGaAsP/InP lasers for polarization stabilization", IEEE J, Quantum Electr. **QE-21** 271 (1985)

[10] Y. Mori,J. Shibata and T.Kajiwara,"Optical polarization bistability in TM wave injected semiconductor lasers", IEEE J. Quantum Electron. **25**(3) 265 (1989)

[11] R. M. Ryan and R. C. Miller, "The effect of uniaxial strain on the threshold current and output of GaAs lasers", Appl. Phys. Lett. **3**(9) 162 (1963)

[12] N. B. Patel, J. E. Ripper, and P. Brosson, "Effects of uniaxial stress on the double heterostructure lasers", IEEE, J. Quantum Electron. **QE-9**(2) 338 (1973)

[13] N.K. Dutta, "Effect of uniaxial stress on optical gain in semiconductors", J. Appl. Phys. **55**(2) 285 (1984)

[14] H. Asai and K. Oe, "Energy band-gap shift with elastic strain in $Ga_xIn_{1-x}P$ epitaxial lasers on (001) GaAs substrates", J. Appl. Phys. **54**(4) 2052 (1983)

[15] T. C. Chong and C. G. Fonstad, "Theoretical gain of Strained-layer semiconductor lasers in the large strain regime", IEEE, J. Quantum. Electr., **25**(2) 171 (1989)

[16] T. Tanbun-EK, N. A. Olsson, R. A. Logan, K. W. Wecht, and A. M. Sergent, "Measurements of the polarization dependent of the gain of strained multiple quantum well InGaAs-InP lasers", IEEE, J. Quantum. Electr., **3**(2) 103 (1991)

[17] C. E. Zah, B. Bhat, B. Pathak, C. Caneau, F. J. Favire N.C. Andreadakis,D.M. Hwang,M.A.Koza,C.Y.Chen,T.P. Lee, "Low threshold 1.5 μm tensile-strained single quantum well lasers", Electron. Letters **27**(16) 1414 (1991)

[18] G.E. Pikus and G.L. Bir, "Effect of deformation on the hole energy spectrum of germanium and silicon", Sov. Phys. Solid State, **1** 1502 (1960)

[19] E. Yablonovitch and E. O. Kane, "Reduction of lasing threshold current density by the lowering of valence band effective mass", J.Lightwave Tech. **4**(5) 504 (1986)

[20] S.L. Chuang, "Efficient band-structure calculations of strained quantum wells", Phys. Rev. **43**(12) 9649 (1991)

[21] See, for example, reference [**14**] or [**17**]

[22] See references [**16**] and [**17**]. Be careful with the definition of HH(heavy hole) and LH(light hole).

[23] R. F. Pierret, **Advanced Semiconductor Fundamentals**, Modular series on solid state device **VI**, Addison-Wesley Publish Comp. (1987)

[24] C. M. Wolfe, N. Holonyyak, and G. E. Stillman, **Physical Properties of Semiconductors**, Prentice Hall, (1989)

[25] S. Gasiorowicz, **Quantum Physics**, John Wiley & Sons, Inc. (1974)

[26] G.P. Agarwal and N.K. Dutta, **Long-Wavelength Semiconductor Lasers**, Van Nostrand Teinhold Inc.(1986)

[27] R. H. Yan, S. W. Corzine, L.A. Coldren, and I. Suemune, "Corrections to the expression for gain in GaAS", IEEE J. Quantum Electron. **26**(2) 213 (1990)

[28] Y. Lam, J.P. Loehr, and J. Singh,"Comparison of steady-state and transient characteristics of lattice-matched and strained InGaAs-AlGaAs (on GaAs) and InGaAs-AlInAs (on InP) quantum-well lasers", IEEE J. Quantum Electron. **28**(5) 1248 (1992)

[29] J.T. Verdeyen, **Laser Electronics**, Prentice-Hall, (1989)

[30] M. Asada and Y.Suematsu,"Density-matrix theory of semiconductor lasers with relaxation broadening model-gain and gain-suppression in semiconductor lasers", IEEE J. Quantum Electron. **QE-21**(5) 434 (1985)

[31] M. Sargent, M.O. Scully, and W.E. Lamb, **Laser Physics** Addison-Wesley Publishing Company (1974)

[32] G. Dresselhaus, A. F. Kip, and C. Kittel, "Cyclotron resonance of electrons and holes in silicon and germanium crystals", Phys. Rev. **98**(2) 368 (1955)

[33] J. M. Luttinger and W. Kohn, "Motion of electrons and holes in perturbed periodic fields", Phys. Rev. **97**(4) 869 (1955)

[34] C. Kittel, **Quantum Theory of Solid**, John Wiley & Sons (1987)

[35] A. Anselm, **Introduction to Semiconductor Theory**, Mir Publishers and Prentice-Hall, Inc, (1981)

[36] G. Dresselhaus, "Spin-Orbit coupling effects in zinc blende structure", Phys. Rev. **100** 580 (1955)

[37] L. Schiff, **Quantum Mechanics**, McGraw-Hill, New York (1955)

[38] L. Landau and W. Lifshitz, **Quantum Mechanics**, Addison-Wesley (1958)

[39] E. O. Kane, "Band structure of indium antimonide", J. Phys. Chem. Solids., **1** 249 (1957)

[40] S. Datta, **Quantum Phenomena**, Modular series on solid state devices, Addison-Wesley Pub. Inc. (1989)

[41] Numerical Data and Functional Relationships in Science and Technology, edited by K. H. Hellwege et al., New Series, Group III Vol. **17a** (Springer Berlin,1982); Group III-V, Vol. **22a** (Springer Berlin, 1986)

[42] J.C. Hensel and G. Feher, "Cyclotron resonance experiments in uniaxially stressed silicon: valence band inverse mass parameters and deformation potentials", Phys. Rev. **129**(3) 1041 (1963)

[43] Pollak, **Strained-layer: Physics**, (Semiconductors and Semimetals Vol. 32 by T. P. Pearsall, Academic Press, Inc. (1990)

[44] D.Q. Fletcher, **Mechanics of Materials**, CBS College Publishing (1985)

[45] G. R. Buchanan, **Mechanics of Materials**, Holt, Rinehart and Winston, Inc., (1990)

[46] E. Oomura Et. al., "InGaAsP/InP Buried Crescent Laser Diode Emitting at 1.3 μm Wavelength", IEEE J. Quantum Electronics, **QE-20**(8) 866 (1984)

[47] C. S. Adams, **Stress Dependent Behaviour of InGaAsP Semiconductor Diode Lasers**, McMaster University

[48] **Newport Catalog Book**, Newport Corporation (1990)

[49] C. Sheng and D.T. Cassidy, "Effect of Strain on the Below-Threshold Output of InGaAsP Diode Lasers", in **Abstract of NRC Sixth Canadian Semiconductor Technology Conference**, (1992)